Defect engineering in GaAs using high energy light ion irradiation: Role of electronic energy loss

D. Kabiraj[1] and Subhasis Ghosh[2,a)]
[1]*Inter-University Accelerator Centre, Aruna Asaf Ali Marg, New Delhi 110067, India*
[2]*School of Physical Sciences, Jawaharlal Nehru University, New Delhi 110067, India*

(Received 30 June 2010; accepted 3 December 2010; published online 1 February 2011)

We report on the application of high energy light ions (Li and O) irradiation for modification of defects, in particular, for annihilation of point defects using electronic energy loss in GaAs to minimize the defects produced by nuclear collisions. The high resolution x-ray diffraction and micro-Raman spectroscopy have been used to monitor that no lattice damage or amorphization take place due to irradiating ions. The effects of irradiation on defects and their energy levels have been studied using thermally stimulated current spectroscopy. It has been observed that till an optimum irradiation fluence of 10^{13} ions/cm^2 there is annihilation of native defects but further increase in irradiation fluence results in accumulation of defects, which scales with the nuclear energy loss process, indicating that the rate of defects produced by the binary collision process exceeds rate of defect annihilation. Defect annihilation due to electronic energy loss has been discussed on the basis of breaking of bonds and enhanced diffusivity of ionized native defects. © *2011 American Institute of Physics*. [doi:10.1063/1.3534003]

I. INTRODUCTION

Low energy ion implantation is the method of choice in semiconductor manufacturing for doping due to its ability to control the number of implanted dopants and to place them at the desired depth. The energy of the ions used for the purpose of implantation is in the range of few kilo-electron-volts to few hundred kilo-electron-volts. The defects produced in these energies are mostly by nuclear energy loss. The mechanism of creation and annihilation of defects by this binary collision process is fairly understood.[1] Recently, ion implantation with much higher energy (approximately mega-electron-volts) has attracted considerable attention[2] as it provides an extension of ion implantation technique much deeper inside the semiconductor and for three-dimensional electronic device fabrication and fabrication of nanostructures. Extending the ion energy from kilo-electron-volts to mega-electron volts provides many advantages in terms of the larger ion range for deep implantation and the minimized surface damage[3] for modification of deeply buried layers. Until now high energy heavy ions (HEVI) have been used for understanding the ion-matter interaction and application in the areas of deep buried layer and materials modifications.[4–7] In this case nuclear energy loss and/or localized intense electronic energy loss is predominantly responsible for material modifications through formation of latent tracks. But the role of high energy light ions (HELI) irradiation for materials modifications have not been explored much. There are several advantages of HELI over HEVI. In contrast to HEVI, energy loss by HELI is mostly by electronic ($\geq$99%) and the rest by nuclear process. The nuclear energy loss process is efficient in producing defects by the binary collision. During electronic energy loss process energy is transferred between the incident particle and free and bound electrons in the target, ionizing target atoms, create energetic electrons and electronic spike causing local heating. The interaction of HELI with materials is unique in the context of defect engineering because HELI irradiation introduce very low structural damage due to low nuclear energy loss but high electronic energy loss produces localized heating, bond breaking, and enhanced defect annealing by lowering diffusion activation energy of defects.[8] There are several reports[3,9–11] on HEVI induced track like extended defect formation in GaAs, created by highly localized ionized zone due to electronic energy loss process. But there is not much to report on the effects of HELI irradiation in the context of engineering of defects in GaAs. Nevertheless, there are few investigations using HELI such as Kuriyama *et al.*[12] have studied the quenching phenomena of photoconductance related to the EL2 defect in 15 MeV proton irradiated semi-insulating (SI)-GaAs. Recently, it has been shown that electrically active defects produced in Si along ion track can result in a pinning of the Fermi level to a dominant deep level such as the divacancy (V_2).[13,14] This occurs within a region of $<$100 nm around an ion track and results in formation of a nanosized channel with a modified Fermi level embedded in bulk Si.

II. EXPERIMENT

In this study SI-GaAs samples were irradiated by 50 MeV Li and 100 MeV O with fluences ranging between 10^{12} and 10^{14} ions/cm^2 using 16UD Pelletron facility at Inter-University Accelerator Centre, New Delhi. The samples were also irradiated by 1.5 keV Ar beam at a fluence of 10^{16} ions/cm^2. The energies of the ions were chosen such that the velocities are approximately the same for both the ions to eliminate the velocity effect[1] on damage production. In this study HELI irradiated SI-GaAs samples have been characterized using thermally stimulated current spectros-

a)Electronic mail: subhasis@mail.jnu.ac.in.

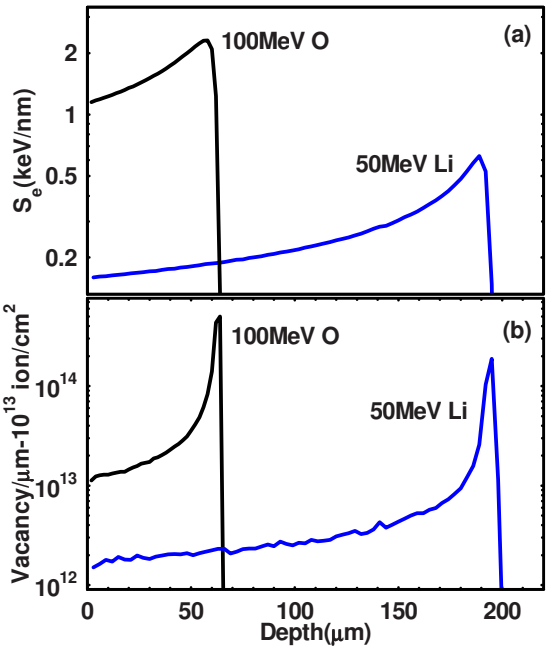

FIG. 1. (Color online) (a) The depth vs electronic energy loss inside GaAs samples calculated using TRIM simulation for 50 MeV Li and 100 MeV O. (b) The result of TRIM simulation for the depth distribution of the vacancy density in the GaAs sample irradiated with 10^{13} ions/cm^2 of 50 MeV Li and 100 MeV O ions.

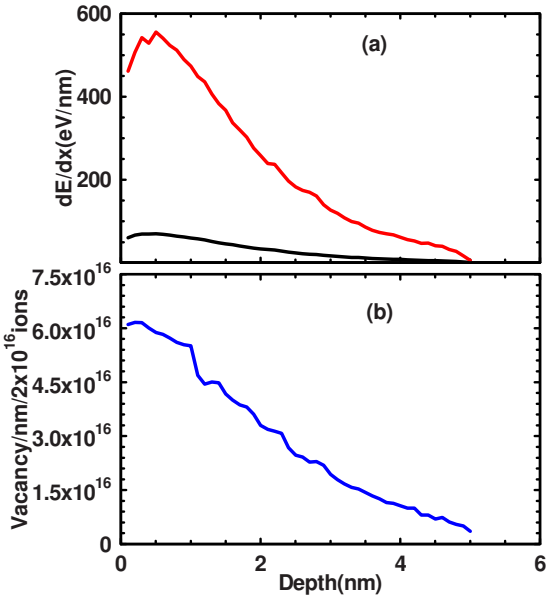

FIG. 2. (Color online) (a) TRIM simulation of depth distribution of S_e (black line) and S_n (red line) due to 1.5 keV Ar irradiation in GaAs and (b) vacancy distribution produced by 2×10^{16}, 1.5 keV Ar in GaAs.

copy (TSCS).[15] The range of the Li and O ions in GaAs are 200 μm and 71 μm, respectively. In most cases, the thickness of the sample is less than the range of the ions. The energy loss of HELI is mainly due to electronic process (0.2–1.1 keV/nm) and rest by nuclear process (0.09–0.7 eV/nm), which is three orders of magnitude lower than electronic energy loss. The depth versus electronic energy loss inside GaAs samples calculated using TRIM (Ref. 1) simulation for 50 MeV Li and 100 MeV O and shown in Fig. 1(a). Similarly for 1.5 keV Ar the depth versus electronic and nuclear energy loss are shown in Fig. 2(a). To ensure that the defects are not related to irradiation induced surface damage, 3 μm of the sample surface was etched out prior to TSCS measurement. No surface damage related effect could be detected. We have performed TRIM simulation to estimate the depth distribution of vacancies produced by irradiating ions. Figure 1(b) shows that the depth distribution of vacancies is uniform within 40 μm and 100 μm in case of O and Li, respectively. Figure 2(b) shows the same for 1.5 keV Ar. It is estimated that each of the 50 MeV Li and 100 MeV O produce 14 and 123 vacancies, respectively, showing minimum average distance between the defects produced is approximately 160 nm. This indicates that interaction between defects is not possible which are produced along an ion path, thus production of point defects is only expected. In contrast to high energy ions, 1.5 keV Ar lose maximum energy by nuclear energy loss process (336 eV/nm) and much less, 41 eV/nm, due to electronic energy loss. The TRIM simulations show that the range of the ions in GaAs is 3 nm and approximately 17 vacancies are produced per Ar bombardment [Fig. 2(b)]. Ohmic contacts were prepared by thermal evaporation of AuGe/Ni/Au and subsequent annealing at 400 °C. In order to perform the TSCS under identical initial conditions, the following sequence was used: (i) the sample was cooled to 10 K in the dark and equilibrated for 2 h and then photoexcited by 1.37 eV photons for trap filling and finally illumination was terminated for obtaining the TSCS spectra from 10 to 300 K by heating the sample at the rate of 0.1 K/s; (ii) the temperature was raised to 320 K and equilibrated for 2 h to ensure that the defect levels are unoccupied; (iii) then brought down to 10 K and step (i) was followed. The intensity and duration of illumination were kept the same for all the measurements.

III. RESULTS AND DISCUSSION

A. TSCS results at low fluence: Annealing of defects

Figures 3 and 4 show the results of TSCS spectra of the samples irradiated by 50 MeV Li and 100 MeV O, respectively, at various fluences. From these two figures we observe that there is reduction in TSC peak at 20 K which is related to metastable state of EL2 in the samples irradiated by Li and O with 10^{12} ions/cm^2.[16] The most interesting feature is the complete annihilation of the peak at 86 K. Further, we observe the annihilation of almost all the shallow levels including the metastable peak at 20 K in the samples irradiated with 10^{13} ions/cm^2 of O and 10^{14} ions/cm^2 of Li.

B. TSCS results at high fluence: Regeneration of defects

As the irradiation fluence exceeds 10^{13} ions/cm^2 there is onset of thermally activated current with lower activation energies due to accumulation of defects created by irradiation. Estimation of activation energy from thermally stimulated current is described elsewhere.[17] In the sample irradiated with 10^{13} ions/cm^2 the activation energy of $\sim$750 meV is recorded, which is due to EL2 related defects in GaAs. But in the sample irradiated with 10^{14} ions/cm^2 Li there is onset of thermally activated current with activation

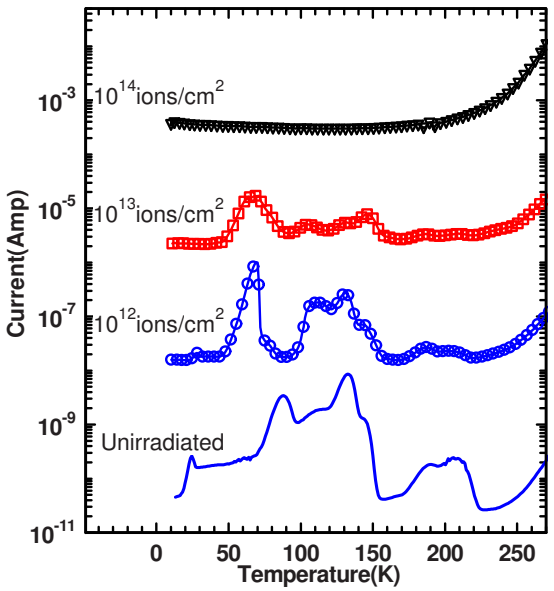

FIG. 3. (Color online) TSC spectra of unirradiated sample and samples irradiated with 50 MeV Li at different fluences of 10^{12}, 10^{13}, and 10^{14} ions/cm^2. The spectra are shifted vertically for clarity.

energy of 200 meV, and it is 145 meV and 120 meV in the sample irradiated with 5×10^{13} ions/cm^2 and 10^{14} ions/cm^2 of O respectively.

Based on the earlier published results the defect states having activation energy of 120 and 280 meV could be related to V_{As} and a complex related to V_{As},[18–20] whereas the deeper levels are related to antisite defects of GaAs.[21–24] The results of annealing of the irradiated samples show that annealing of the defects take place at 400 °C, which ensures that complex defects are not produced due to irradiation, only V_{As}-As_i type defects are produced which we have already reported.[17]

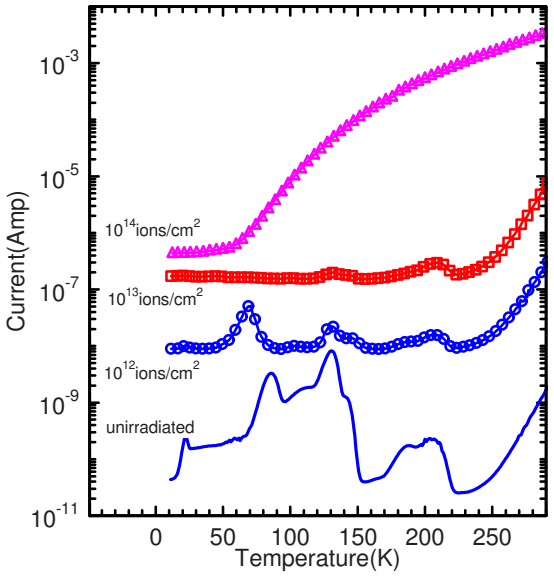

FIG. 4. (Color online) TSC spectra of unirradiated sample and samples irradiated with 100 MeV O at different fluences of 10^{12}, 10^{13}, 5×10^{13}, and 10^{14} ions/cm^2. The spectra are shifted vertically for clarity.

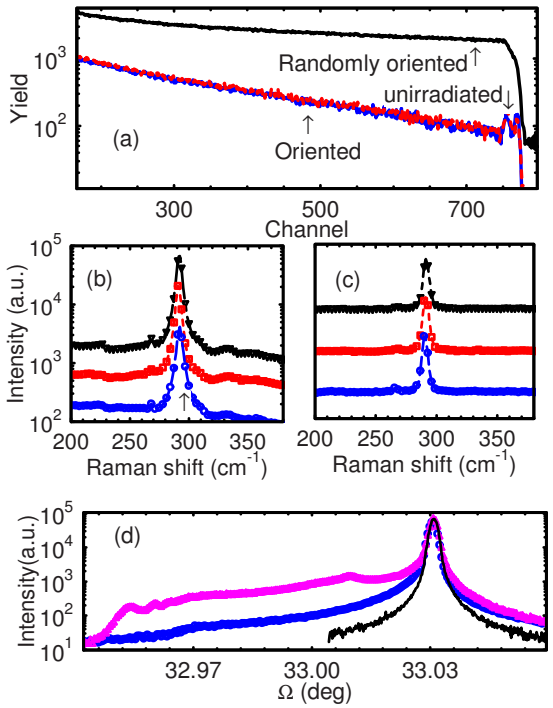

FIG. 5. (Color online) (a) c-RBS spectra of unirradiated and irradiated GaAs. The backscattered yield is shown for (i) randomly oriented unirradiated GaAs and (ii) oriented GaAs irradiated with 100 MeV O at a fluence of 1×10^{14} ions/cm^2. The two peaks indicated by ↓ are due back scattered He from Ga and As atoms at the GaAs surface. (b) Raman spectra of GaAs samples. Unirradiated (○), irradiated by 100 MeV O with 10^{13} ions/cm^2 (□) and 10^{14} ions/cm^2 (▽). The spectra are shifted vertically for clarity. The LO mode at 295 cm^{-1} is shown by arrow (↑). (c) Raman spectra of unirradiated (○), irradiated by 50 MeV Li with 10^{13} ions/cm^2 (□) and 10^{14} ions/cm^2 (▽). The spectra are shifted arbitrarily along the y-axis for better visualization. (d) HRXRD $I(\Omega)$ plot of unirradiated (solid line) sample, sample irradiated by 100 MeV O with 10^{14} ions/cm^2 (△) and 50 MeV Li with 10^{14} ions/cm^2 (○).

C. Structural characterization

The channeling-Rutherford backscattering spectroscopy (c-RBS) and micro-Raman spectroscopy were carried out on the unirradiated and irradiated samples. No apparent change in the c-RBS and Raman spectrum of unirradiated sample and sample irradiated by 100 MeV O with 10^{14} ions/cm^2 as shown in Figs. 5(a) and 5(b). Figure 5(c) shows the Raman spectrum of unirradiated sample and sample irradiated by 50 MeV Li. They indicate that amorphization has not taken place due to irradiation. The high resolution x-ray diffraction (HRXRD) was carried out using Bruker D8 Discover High-Resolution diffractometer. Rocking curves were measured at the (004) reflection, which is very sensitive to strain in the vertical layer structure. The x-ray penetration depth in this case is larger than 5 μm. The (004) rocking curves of unirradiated sample and the samples irradiated by Li and O at fluences of 10^{14} ions/cm^2 are shown in the inset of Fig. 4. The reflected x-ray peak of the unirradiated sample has nearly Gaussian shape and full width at half maximum (FWHM) of 0.002°, which is a typical value for GaAs measured with the configuration described above.[25] It is evident from the figure that irradiation induced compressive strain due to expansion of lattice has developed in irradiated samples.

1. Role of electronic energy loss

The TSCS measurements indicate that there is annihilation of defects till an optimum fluence of 10^{13} ions/cm^2, and beyond this fluence accumulation of defects takes over annihilation, which results in degradation of samples. In our previous report[26] it was shown that the role of ionization created by electronic energy loss process is to produce various defects in their higher charge states. The ionization may also promote annealing of defects.

The concentration of EL2 defects in LEC grown GaAs is approximately 5×10^{16}/cm^3. The density of other defects which contribute to the TSC spectrum in approximately 5×10^{15}/cm^3.[27] Considering a 20 μm thick slab of area 1 cm^2, GaAs contains approximately 10^{21} of Ga and As atoms and 10^{14} of defects which contribute to TSC peaks. Within this volume the binary collisions between 10^{13} of 100 MeV O and Ga and As atoms produce approximately 1.2×10^{15} of Ga and As vacancies and interstitials stochastically with equal probability. Out of which the defects produced in Ga sublattice anneal out at room temperature.[28] So, it is very unlikely that the observed annihilation of defects at irradiation fluence of 10^{13} O ions/cm^2 is the result of binary collision process only which is related to nuclear energy loss. We have also observed that there is no change in the room temperature resistivity of GaAs samples irradiated at fluence of 10^{13} ions/cm^2 which indicate that there is no change in charge compensation.[18] The compensation in undoped SI-GaAs is achieved by introduction of deep donor EL2 defects with a concentration of approximately 10^{16}–10^{17}/cm^3 during growth process. The deep donor defect EL2 compensates holes contributed by unwanted shallow carbon acceptors. The unchanged resistivity of the samples irradiated at 10^{13} ions/cm^2 shows that there is no change is the concentration of EL2 defects due to irradiation. Unchanged EL2 concentration in sample irradiated at 10^{13} ions/cm^2 indicates that nuclear energy loss is not the only cause for the annihilation of defects as observed in the TSC spectrum. Apart from nuclear energy loss, the ions lose most of their energies by electronic process. During electronic energy loss the ions undergo inelastic collisions with bound electrons in the medium. The electrons can be excited to higher energy levels and produce energetic electron known as δ-electrons, or excited in the collective motion of plasmons.[29] In case of 100 MeV O and 50 MeV Li the average energy of the δ-electrons are approximately 1.55 keV and 1.56 keV, respectively, as calculated from the following relation:[30]

$$\varepsilon_m = \frac{\bar{I}(2m_e v^2+\bar{I})}{2m_e v^2}\ln\left(\frac{2m_e v^2+\bar{I}}{\bar{I}}\right)-\bar{I}, \quad (1)$$

where $\bar{I}$ is the mean ionization potential, which is approximately 325 eV for Ga and As.[31] These electrons are ejected outwards from ion trajectory leaving behind a cylindrical zone of influence restricted by the energy of the electrons. A schematic representation shows the interaction of HELI with lattice during the passage through a sample in Fig. 6, which shows the trajectories of δ-electrons and the region of influence around an ion path. The range of 10 keV electron in GaAs is approximately 1 μm,[32] the δ-electrons which are produced by 100 MeV O can cover an area of influence with radius of 155 nm. It has been shown[30] that primary beam along with the δ-electrons promote defect annihilation through ionization and/or breaking bonds. Ionization process has a large role to play in various aspects of defect engineering and materials modifications. It has been shown that there is enhancement in epitaxial crystallization of preamorphized Si due to inelastic electronic scattering of ions with mega-electron-volt energy.[33] The enhancement in the crystallization is described due to inelastic collision induced charged vacancies, which avoid recombination with interstitial Si atoms in the crystalline substrate due to their higher mobility. Electrons with energies below the threshold displacement energy are shown to be capable of crystallization of isolated amorphous zones in number of elemental and compound semiconductors.[34] The high energy secondary electrons with energies between 1–2 keV which are produced during electronic energy loss can also be efficient for defect annealing. The annealing of latent tracks stimulated by secondary electrons produced through electronic energy loss has been shown to be partly responsible for the observation of unexpectedly low damage cross section in some semiconducting materials.[6] We have shown that[30] the breakup of hydrogen indium vacancy complex $V_{In}H_4$ in Fe doped SI InP by HELI irradiation is due to bond breaking by the secondary electrons. It is reported that ionization-induced spontaneous defect recovery occurs in GaAs due to lowering of activation energy of higher-charge-state interstitials.[35] Also there are some reports on the transformation of EL2 defects from one charge state to another due to high energy proton irradiation.[12,36,37] We have also reported that decrease in photoquenching efficiency of SI-GaAs samples due to irradiation is correlated with annihilation of defect levels related to EL2.[26] But unchanged charge compensation[17] of the irradiated samples indicates that irradiation transforms quenchable EL2 defects to nonquenchable state.

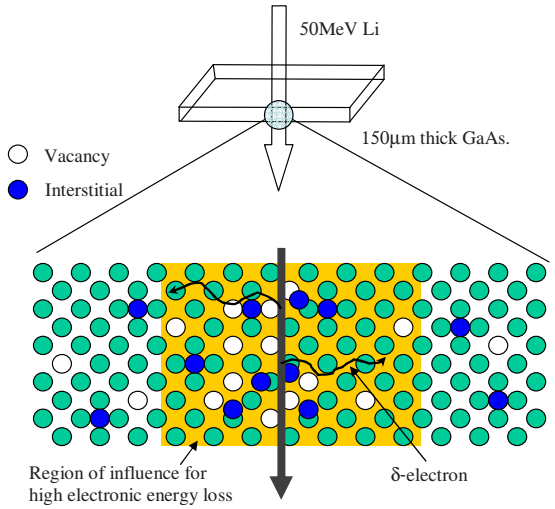

FIG. 6. (Color online) A schematic representation of 50 MeV Li passes through GaAs sample as the thickness of the sample is less than the ion range (~200 μm). The schematic below shows the interaction with lattice during the passage of HELI. The trajectories of δ-electrons and the region of influence around an ion path are shown in the schematic.

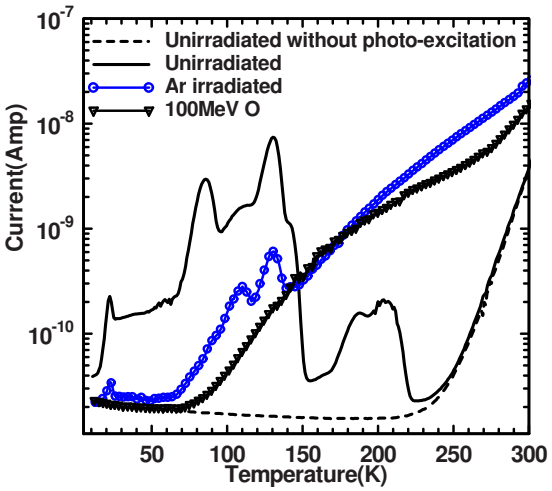

FIG. 7. (Color online) Comparison of TSC spectra unirradiated sample and samples irradiated with 1.5 keV Ar (○), 100 MeV O (▽), and 50 MeV Li (□). The TSC spectra of unirradiated sample recorded without photoexcitation is shown as reference.

2. Role of nuclear energy loss

Irradiation at fluences above 1×10^{13} ions/cm^2 leads to regeneration of some of the annihilated defects as shown in Fig. 4. This may be due to the accumulation of defects produced by nuclear energy loss process after dynamic annealing which takes place in GaAs irradiated at 300 K.[28] At fluence of 3×10^{13} ions/cm^2 the distance between two nearest trajectories becomes approximately 1 nm. The size of GaAs unit cell is 0.565 nm, so above this fluence statistically ion trajectories will pass through each unit cell. To confirm the role of nuclear energy loss in defect accumulation, 1.5 keV Ar irradiation have been performed where energy loss is predominantly due to nuclear energy loss.

Figure 7 shows TSC spectra of the sample exposed to 1.5 keV Ar atom beam. Thickness of the surface layer modified by 1.5 keV Ar ions is close to 3 nm, the thermally stimulated current flow through both modified and unaffected layers. So the spectrum shows the resultant current flowing through the two layers in parallel. We observe that thermally activated current which is flowing in the irradiated region is almost identical to that in the sample irradiated with 5×10^{13} ions/cm^2 of O. It shows that even if the energy of ions differs by several orders of magnitude, the same kinds of defects are produced by nuclear energy loss in GaAs. TRIM calculation also shows that vacancies produced by 100 MeV O and 1.5 keV Ar are approximately the same as 2×10^{16} and 1×10^{17}, respectively, for the respective irradiated fluences.

IV. CONCLUSIONS

In conclusion, we have shown that there is annihilation of defects due to HELI irradiation in SI-GaAs till the ion fluence reaches an optimum value of $\sim10^{13}$ ions/cm^2. It is emphasized that the nuclear energy loss cannot account only annihilation of defects. Defect annihilation by ionization and bond breaking may have been promoted by electronic energy loss. With increasing irradiation fluence there is accumulation of irradiation induced defects which form deep levels in the band gap. c-RBS or LO phonon scattered peak in micro-Raman spectroscopy results show that the samples are not amorphized when irradiated with highest fluence of 10^{14} ions/cm^2. But the HRXRD results show that irradiation has introduced lattice strain. As the irradiation fluence increases, the accumulation of vacancy related defects are observed. With the help of very low energy Ar irradiation we have shown that the defect accumulation due to HELI irradiation at higher fluences is due to nuclear energy loss only.

ACKNOWLEDGMENTS

The authors are thankful to Pelletron group for providing a good-quality scanned beam for irradiation.

[1] J. F. Ziegler, J. P. Biersac, and U. Littmark, *The Stopping and Range of Ions in Matter* (Pergamon, New York, 1985).
[2] J. O. Borland and R. Koelsch, Solid State Technol. **36**, 28 (1993).
[3] W. Wesch, A. Kamarou, and E. Wendler, Nucl. Instrum. Methods Phys. Res. B **225**, 111 (2004).
[4] Amit Kumar, D. K. Avasthi, J. C. Pivin, A. Tripathi, and F. Singh, Phys. Rev. B **74**, 153409 (2006).
[5] S. K. Srivastava, D. K. Avasthi, W. Assmann, Z. G. Wang, H. Kucal, E. Jacquet, H. D. Carstanjen, and M. Toulemonde, Phys. Rev. B **71**, 193405 (2005).
[6] A. Kamarou, W. Wesch, E. Wendler, A. Undisz, and M. Rettenmayr, Phys. Rev. B **73**, 184107 (2006).
[7] C. S. Schnohr, P. Kluth, R. Giulian, D. J. Llewellyn, A. P. Byrne, D. J. Cookson, and M. C. Ridgway, Phys. Rev. B **81**, 075201 (2010).
[8] F. Xiong, C. J. Tsai, T. Vreeland, Jr., T. A. Tombrello, C. L. Schwartz, and S. A. Schwartz, J. Appl. Phys. **69**, 2964 (1991).
[9] W. Wesch, A. Kamarou, E. Wendler, and S. Klaumunzer, Nucl. Instrum. Methods Phys. Res. B **242**, 363 (2006).
[10] R. Lauck, E. Wendler, and W. Wesch, Nucl. Instrum. Methods Phys. Res. B **242**, 484 (2006).
[11] A. Colder, B. Canut, M. Levalois, P. Marie, X. Portier, and S. M. M. Ramos, J. Appl. Phys. **91**, 5853 (2002).
[12] K. Kuriyama, H. Takahashi, H. Kawahara, N. Hyahashi, H. Wanatabe, I. Sakamoto, and I. Kohno, J. Appl. Phys. **68**, 6517 (1990).
[13] L. Vines, E. Monakhov, B. G. Svensson, J. Jensen, A. Hallén, and A. Yu. Kuznetsov, Phys. Rev. B **73**, 085312 (2006).
[14] L. Vines, E. V. Monakhov, J. Jensen, A. Yu. Kuznetsov, and B. G. Svensson, Phys. Rev. B **79**, 075206 (2009).
[15] D. C. Look, Semicond. Semimetals **19**, 75 (1983).
[16] D. Kabiraj and S. Ghosh, Appl. Phys. Lett. **87**, 252118 (2005).
[17] D. Kabiraj, R. Grötzschel, and S. Ghosh, J. Appl. Phys. **103**, 053703 (2008).
[18] Z.-Q. Fang and D. C. Look, J. Appl. Phys. **73**, 4971 (1993).
[19] D. C. Look, Z.-Q. Fang, J. W. Hemsky, and P. Kengkan, Phys. Rev. B **55**, 2214 (1997).
[20] M. Pavlović, U. V. Desnica, and J. Gladić, J. Appl. Phys. **88**, 4563 (2000).
[21] K. Sarrinen A. P. Seitsonen, P. Hantojarvi, and C. Corbel, Phys. Rev. B **52**, 10932 (1995).
[22] H. Seong and L. J. Lewis, Phys. Rev. B **52**, 5675 (1995).
[23] J. T. Schick, C. G. Morgan, and P. Papoulias, Phys. Rev. B **66**, 195302 (2002).
[24] Y. Oyama and J. Nishizawa, J. Appl. Phys. **97**, 033705 (2005).
[25] U. Zeimer and E. Nebauer, Semicond. Sci. Technol. **15**, 965 (2000).
[26] D. Kabiraj and S. Ghosh, Semicond. Sci. Technol. **20**, 1022 (2005).
[27] S. Kuisma, K. Saarinen, P. Hautoaarvi, Z. Q. Fang, and D. C. Look, J. Appl. Phys. **81**, 3512 (1997).
[28] W. O. Siyanbola and D. W. Palmer, Phys. Rev. Lett. **66**, 56 (1991).
[29] G. Schiweitz, K. Czerski, M. Roth, F. Staufendiel, and P. L. Grande, Nucl. Instrum. Methods Phys. Res. B **226**, 683 (2004).
[30] D. Kabiraj, A. Roy, J. C. Pivin, and S. Ghosh, J. Appl. Phys. **104**, 033711 (2008).
[31] S. P. Ahlen, Rev. Mod. Phys. **52**, 121 (1980).
[32] *Electron-Beam Technology in Microelectronic Fabrication*, edited by G. Brewer (Academic, New York, 1980).
[33] J. Nakata, J. Appl. Phys. **79**, 682 (1996).

[34]I. Jenčič, E. P. Hollar, and I. M. Robertson, Philos. Mag. **83**, 2557 (2003).
[35]D. Stievenard, X. Boddaert, J. C. Bourgoin, and H. J. von Bardeleben, Phys. Rev. B **41**, 5271 (1990).
[36]R. Ferrini, M. Galli, M. Patrini, F. Nava, C. Canali, and P. Vanni, Appl. Phys. Lett. **71**, 3084 (1997).
[37]M. Rogalla, M. Battke, N. Duda, R. Geppert, R. Goeppert, R. Irsigler, J. Ludwig, K. Runge, Th. Schmid, W. Joerger, and K. W. Benz, Nucl. Instrum. Methods Phys. Res. B **134**, 53 (1998).